Nuclear Engineering and Design 329 (2018) 46–52

Contents lists available at ScienceDirect

Nuclear Engineering and Design

journal homepage: www.elsevier.com/locate/nucengdes

Silicon carbide grain boundary distributions, irradiation conditions, and silver retention in irradiated AGR-1 TRISO fuel particles

T.M. Lillo[a,*], I.J. van Rooyen[b], J.A. Aguiar[b]

[a] Materials Science and Engineering Department, Idaho National Laboratory, PO Box 1625, Idaho Falls, ID 83415-2211, USA
[b] Fuel Design and Development Department, Idaho National Laboratory, PO Box 1625, Idaho Falls, ID 83415-6188, USA

ABSTRACT

Distributions of silicon carbide grain boundary types (random high angle, low angle, and coincident site lattice-related boundaries), were compared in irradiated tristructural isotropic-coated fuel particles from the Advanced Gas Reactor-1 experiment exhibiting high (> 80%) and low (< 19%) Ag-110m retention. Grain orientation from transmission electron microscope-based precession electron diffraction data, and, ultimately, grain boundary distributions, indicate irradiated particles with high Ag-110m retention correlate with lower relative fractions of random, high-angle grain boundaries. An inverse relationship between the random, high-angle grain boundary fraction and Ag-110m retention was found and is consistent with grain boundary percolation theory. Also, the SiC grain boundary distribution in an irradiated, low Ag-110m retention, Variant 1 particle was virtually identical to that of a previously reported as-fabricated (unirradiated) Variant 1 TRISO particle. Thus, SiC layers with grain boundary distributions associated with low Ag-110m retention may have developed during fabrication and were present prior to irradiation, assuming significant microstructural evolution did not occur during irradiation. Finally, irradiation levels up to 3.6×10^{25} n/m^2 and 16.7% fissions per initial metal atom were found to have little effect on association of fission product precipitates with specific grain boundary types in particles exhibiting between 19% and 80% Ag-110m retention.

1. Introduction

The silicon carbide (SiC) layer of tristructural isotropic (TRISO)-coated fuel for advanced, high-temperature nuclear reactors acts as the primary barrier for containment of fission products. Although fission product retention during irradiation and safety tests is highly effective (Demkowicz et al., 2015), a significant number of instances have been documented in which Ag-110m is released through seemingly intact SiC layers (Demkowicz et al., 2016; Nabielek and Brown, 1975; Nabielek et al., 1977; Minato et al., 1990; Engelhard et al., 1975). The search for a fundamental microstructural explanation of this behavior has spanned 40+ years and has resulted in a multitude of theories (Van Rooyen et al., 2014; Lillo et al, 2015; Van Rooyen et al., 2014; Maclean, 2004; Van Rooyen et al., 2014; Coward et al., 2015; Van Rooyen et al., 2014; Van Rooyen et al., 2014), which have not been verified in TRISO fuel particles under expected irradiation conditions even though there have been observations from out-of-pile experiments designed to explore this phenomenon.

There is a growing consensus within the community that grain boundary diffusion plays a significant role in both fission product transport and subsequent fission product precipitate formation in irradiated polycrystalline, beta-SiC of near theoretical density, the form exclusively present in TRISO fuel particles (Malherbe, 2013; O'connell et al, 2014; Lòpez-Honorato et al., 2010; Rabone and Lòpez-Honorato, 2015; Deng et al., 2015). In general, grain boundaries exhibit a wide range of diffusivities dependent on the atomic structure at the grain boundary (Balluffi, 1982; Sutton and Vitek, 1983). The exact atomic configuration at the grain boundary is determined by the crystallographic misorientation across the grain boundary and the grain boundary habit plane (Peterson, 1983; Randle, 1997; Wolf, 1990; Herrmann et al., 1976). Also, the grain boundary habit plane is not necessarily linear, but is typically a curved interface and the grain boundary habit plane, and, thus, the atomic configuration at the interface, is continually changing along the length of the boundary. This same interface atomic configuration determines whether the boundary will be of relatively high or low energy as discussed in detail by Dholabhai et al. (2015) and Wu et al. (2015). High-energy grain boundaries (e.g., random, high-angle grain boundaries) exhibit considerably higher grain boundary diffusivities than low-energy boundaries (e.g., coherent twin boundaries). In fact, recent kinetic Monte

* Corresponding author.
E-mail address: thomas.lillo@inl.gov (T.M. Lillo).

https://doi.org/10.1016/j.nucengdes.2017.11.048
Received 27 April 2017; Received in revised form 26 October 2017; Accepted 28 November 2017
Available online 06 December 2017

Carlo simulations (Lòpez-Honorato et al., 2010) show that differing grain boundary networks with differing fractions of high and low-energy grain boundaries could contribute to the observed large variability in the effective silver diffusivity within the SiC layer of TRISO-coated particles reported in literature (see Malherbe (2013) for a review of the data). Similarly, Deng et al. (2015) and O'connell et al. (2014) concluded that neutron fluence and temperature may play a significant role in the transport of silver across the SiC layer in TRISO fuel.

In this study, release behavior and grain boundary distributions of irradiated TRISO particles exhibiting different levels of silver retention, compact burnup and time-averaged, volume-averaged (TAVA) temperatures during the Advanced Gas Reactor (AGR)-1 experiment in the Advanced Test Reactor at Idaho National Laboratory are compared. The influence of neutron irradiation on grain boundary distributions is also discussed.

2. Experimental procedure

The AGR-1 TRISO fuel particles examined in this study were fabricated at Oak Ridge National Laboratory using the baseline and Variant 1 coating conditions. (The fuel kernel was UCO, as opposed to UO_2. However, fuel kernel type is not expected to be a contributing factor in Ag transport in the SiC layer.) Only differences in the coating conditions for the inner pyrolytic carbon (IPyC) layer existed between the two particle variants in this study. The coating conditions for the SiC layer were nominally the same for both baseline (Hunn et al., 2006a) and Variant 1 (Hunn et al., 2006b) particles; therefore, coating conditions were not considered further when interpreting the comparative results.

The TRISO particles analyzed in this work came from compacts of particles that were subjected to the irradiation conditions and characteristics shown in Table 1. The burnup, neutron fluence, and TAVA irradiation temperature in Table 1 are average values for the *compact* of TRISO particles and actual values for individual particles, except neutron fluence, can be significantly different, depending on their location within the cylindrical compact (Hawkes et al., 2014). Since the particle location in the compact could not be determined and tracked, the actual irradiation parameters for each individual particle are unknown. The sample set consisted of one baseline particle exhibiting relatively high retention (80%) for Ag-110m based on post-irradiation gamma spectroscopy scans (AGR1-632-035) and two Variant 1 particles, with one showing complete Ag-110m retention (AGR1-531-031) and one showing relatively low retained amounts (< 19%) of Ag-110m (AGR1-531-038), as shown in Table 1.

Transmission electron microscope (TEM) samples from the SiC layer, which was about 35 μm thick, were produced from a polished cross section of each particle using standard focused ion beam techniques. Fig. 1a shows the general area were samples were taken from the SiC layer of AGR1-531-031, as an example. Sub-areas, Fig. 1b, representing a region near the IPyC/SiC interface (referred to as inner samples because it was nearest the uranium oxycarbide kernel), the central region of the SiC layer (approximately equi-distant from the IPyC and the outer pyrolytic carbon layers), and from the region near the SiC/outer pyrolytic carbon interface (referred to as the outer sample) were taken from the general area in Fig. 1a. Substantial overlap

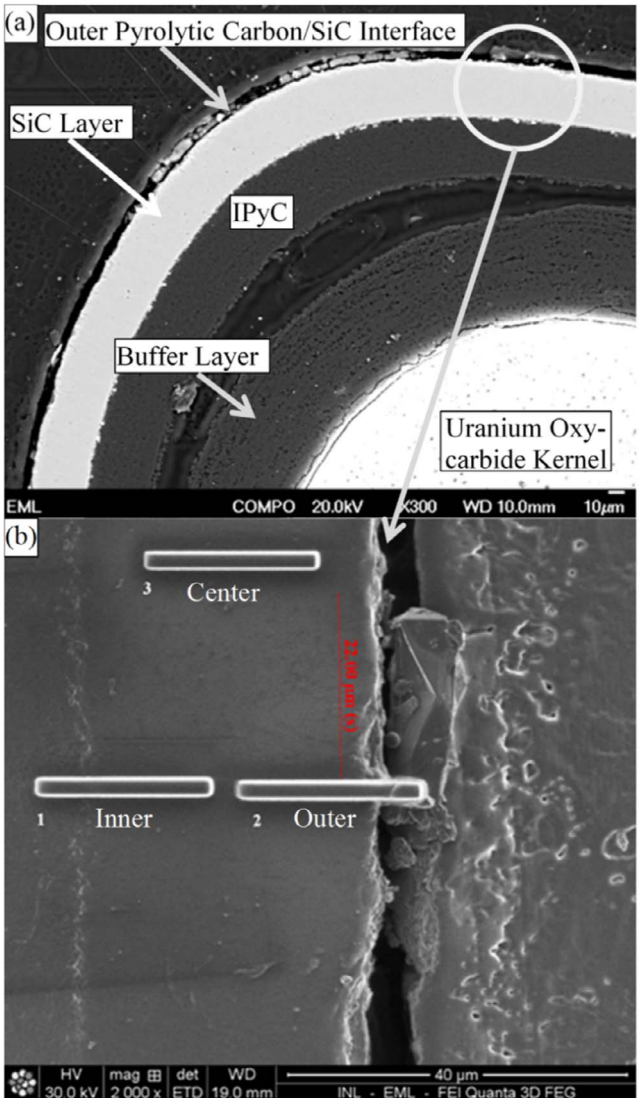

Fig. 1. (A) Overview of the area of the SiC layer that was analyzed in AGR1-531-031 and (b) locations of the inner, center, and outer focused ion beam-extracted TEM samples taken from this area that span the SiC layer.

exists between the samples of these three regions (Fig. 1b).

Multiple areas on the inner, center and outer samples were analyzed and each area contained more than 1000 grain boundaries. The standard error in the grain boundary distributions was determined by dividing the standard deviation for each measured value of grain boundary type (low angle, random high angle, CSL value or misorientation angle) by the square root of the number of areas analyzed, i.e., number of observations, to yield the standard error and the standard error bars in the plots that follow.

Grain boundary distributions within the SiC layer were determined

Table 1
TRSIO particle characteristics and average compact irradiation conditions (Demkowicz et al., 2015).[1]

Particle ID	Fuel Variant	Ag Retention %	Burnup[a], % FIMA	Neutron Fluence[c], $\times 10^{25}$ n/m^2	TAVA[a], °C
AGR1-632-035	Baseline	80	11.4	2.6	1070
AGR1-531-031	Variant 1	105[b]	16.7	3.6	1040
AGR1-531-038	Variant 1	< 19	16.7	3.6	1040

[a] Average values associated with the compact – actual particle conditions may be significantly different.
[b] Estimates of Ag retention are based on the measured inventory divided by the predicted inventory (Demkowicz et al., 2016).[2]
[c] E > 0.18 MeV.

using SiC orientation information gathered from precession electron diffraction (PED) data in the TEM (Tecnai TF30-FEG STwin, operating at 300 kV, at the Center for Advanced Energy Studies) using the ASTAR system (NanoMegas, Inc.). An electron probe size of about 5 nm, in conjunction with a 10-nm step size, was used to collect crystallographic orientation data. The crystallographic information was exported and analyzed using EDAX OIM v7.1.0 software. Two data cleanup routines were applied to all data and consisted of the following:

1. Grain dilation: grain tolerance angle of 2° and minimum grain size of 5 pixels.
2. Neighbor orientation correlation: Grain tolerance set at 2° and minimum confidence index is 0, with a cleanup level of 1. For a cleanup level of 1, all but one of the nearest neighbor data points must share a like orientation before the data point in question will be changed to the same orientation of the nearest neighbors. Data points were collected in a hexagonal pattern; therefore, five of the six nearest neighbors were required to have the same orientation before the orientation of the data point was changed to match the five nearest neighbors.

These data cleaning procedures resulted in less than 3% of the data points being affected. This was well below the limit of 10% allowed in Section 12.2 of American Society for Testing and Materials Standard E2627, which provides guidance on data processing of electron backscatter diffraction data in the determination of grain size (ASTM Standard, 2013). Grain boundaries were defined for a misorientation equal to or greater than 2°. The range of coincident site lattice (CSL)-related grain boundaries was defined to include Σ3 through Σ29. An example of fission product precipitates on grain boundaries and triple junctions in AGR1-531-038, with the corresponding crystallographic orientation map is shown in Fig. 2.

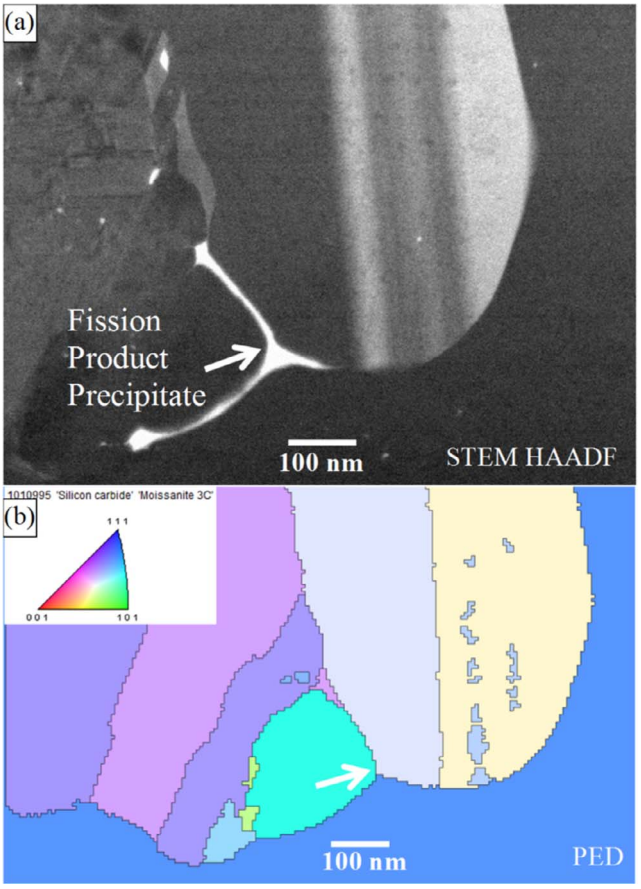

Fig. 2. (A) Example of fission product precipitates on grain boundaries in AGR1-531-038 imaged with atomic contrast scanning transmission electron microscopy with the corresponding orientation map in (b). The same fission product precipitate location is arrowed in each image.

3. Results and discussion

The crystallographic orientation information obtained by PED was analyzed for the following:

1. General grain boundary distributions to explore the relationship between Ag-110m retention behavior (i.e., high or low retention) and grain boundary-type distributions.
2. Comparison of irradiated grain boundary-type distributions with corresponding unirradiated grain boundary type-distributions to explore the influence of irradiation on grain boundary distributions.
3. Compare fission product precipitate/grain boundary-type associations for baseline and Variant 1 TRISO particles and irradiation conditions.

3.1. General grain boundary distributions

Since grain boundaries are considered to have a vital influence on fission product transport through the SiC layer of TRISO fuel during irradiation, orientation mapping and grain boundary statistics provide a way for comparing the three particles in Table 1. Plots comparing grain boundary distributions of three particles are shown in Fig. 3. In general, the particles showing higher Ag-110m retention tend to have more CSL-related grain boundaries than the particle with relatively low Ag-110m retention (Fig. 3a), although the error bars indicate this difference may not be statistically significant. The low-retention particle, AGR1-531-038, also exhibits fewer twin boundaries than the other two higher-retention particles, Fig. 3b (misorientation angle = 60°), and Fig. 3c Σ = 3), although, again, the error bars indicate this difference may not be statistically significant. However, twin boundaries have lower measured diffusivities for impurity atoms (Peterson, 1983; Priester, 1989) and would tend to aid in fission product retention.

Additionally, higher retention of Ag-110m seems to correlate with lower fractions of random, high-angle grain boundaries. Fig. 3a shows that the low Ag retention particle, AGR1-531-038, has statistically more random, high-angle grain boundaries. In fact, a relationship between the Ag-110m retention and the random, high-angle grain boundary fraction is suggested by Fig. 3a.

This relationship is plotted in Fig. 4 and shows an inverse relationship between Ag-110m retention and random, high-angle grain boundary fraction. A linear fit to the data is shown in Fig. 4 and exhibits a relatively good fit ($R^2 = 0.96$), although the error bars on the data from AGR1-0632-035 show considerable overlap with the other two datasets and additional data from other particles should be collected and plotted to verify this relationship.

In addition to the good linear fit to the data, a random, high-angle grain boundary fraction on the order of 48% corresponds to a complete release of Ag-110m at the irradiation temperature of the particles within the duration of the AGR-1 irradiation experiment. This fraction appears to be consistent with grain boundary percolation theory which predicts that below about a fraction of 50%, the interconnected, high diffusivity pathways offered by random, high angle grain boundaries are no longer contiguous throughout the SiC microstructure (Schuh et al., 2003). Fig. 4 indicates that above about 48% random, high-angle grain boundaries, there are enough interconnected, high-diffusivity pathways to allow complete release of Ag-110m within the constraints of the experimental duration and temperature. This figure also indicates a random, high-angle grain boundary fraction of less than approximately 20% would be required to attain complete Ag-110m retention during the AGR-1 irradiation experiment. At a high angle grain boundary fraction of < 20%, there are not enough interconnected high diffusivity pathways to release any Ag-110m within the time at

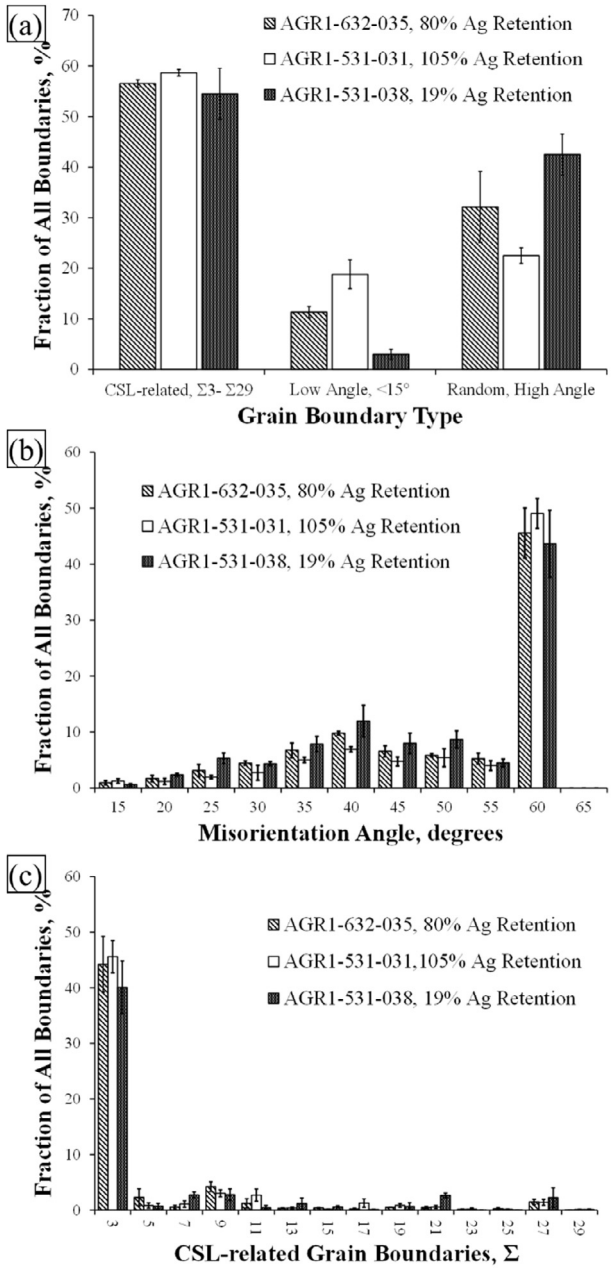

Fig. 3. (A) Plot comparing the distribution by grain boundary type, (b) misorientation angle distribution, (c) coincident site lattice distribution for the three particles.

temperature in the AGR-1 experiment. However, all grain boundaries within the SiC layer have some finite diffusivity for Ag-110m and even a SiC layer with less than 20% random, high angle grain boundaries would eventually exhibit Ag-110m release – even complete release – if the irradiation temperature were high enough and/or the irradiation duration long enough. The implication of Fig. 4 is that a SiC layer with low fractions of random, high angle grain boundaries will retain Ag-110m significantly better than SiC layers with a high fraction of random, high angle grain boundaries for a given irradiation temperature and time.

3.2. Influence of irradiation parameters on grain boundary distributions

The irradiation parameters of temperature and neutron fluence in the AGR-1 experiment were sufficiently high to allow for diffusion to occur, as indicated by the transport of fission products through the SiC layer. Diffusion of Si and C in the SiC layer could potentially result in

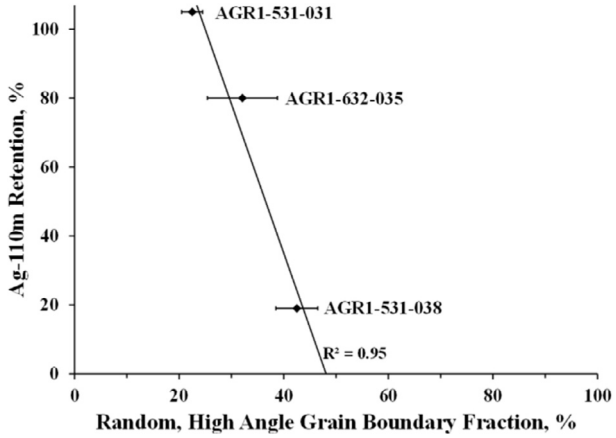

Fig. 4. Correlation between Ag-110m retention and the random, high-angle grain boundary fraction.

significant evolution of the microstructure and changes to the grain boundary distribution. (However, grain growth *without* enhanced diffusion due to neutron damage is not expected because the SiC fabrication temperature was on the order of 1500 °C (Van Rooyen et al., 2012, 2013) and the maximum particle temperature within a compact is expected to be lower than this (Hawkes et al., 2014). Therefore, to assess the potential for SiC microstructural evolution during the AGR-1 experiment, the irradiated SiC grain boundary distributions were compared to the as-fabricated (unirradiated) grain boundary distributions reported by Kirchhofer et al. (2013) (Fig. 5). For the SiC layer

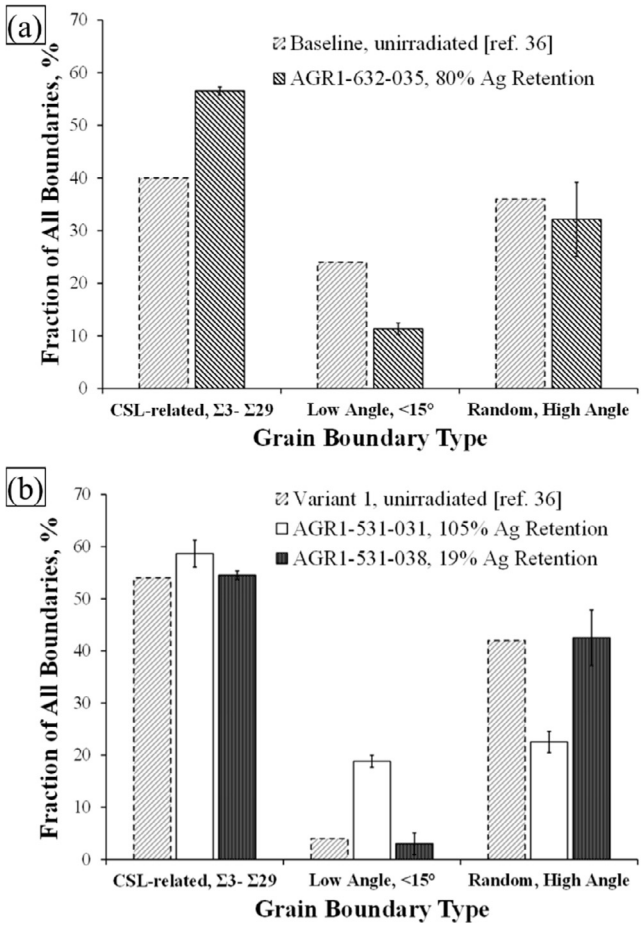

Fig. 5. Comparison of irradiated grain boundary distributions against the unirradiated distributions (as reported in Kirchhofer et al. (2013)): (a) baseline and (b) Variant 1.

fabricated using the baseline fuel fabrication conditions, the unirradiated grain boundary distribution exhibits a larger fraction of low-angle grain boundaries and a lower fraction of CSL-related grain boundaries than the irradiated baseline particle (AGR1-632-035), (Fig. 5a). However, the unirradiated data were collected using scanning electron microscopy-based electron backscatter diffraction with a step size of 50 nm as opposed to the TEM-based PED technique with a 10-nm step size, where the larger step size could result in uniformly dispersed lattice dislocations being interpreted as low angle grain boundaries. (For further discussion of the potential effects of these differences see Lillo et al. (2016).) However, microstructural evolution during irradiation cannot be ruled out as the cause of the differences.

For the Variant 1 comparison, Fig. 5b, the unirradiated grain boundary distribution appears to closely mimic the grain boundary distribution associated with the low Ag-110m retention particle, AGR1-531-038 whereas the distribution associated with the high retention particle, AGR1-531-031, exhibits significantly different low angle and random, high angle grain boundary fractions. If the grain boundary distribution is truly responsible for the Ag-110m release behavior and the temperature of the two irradiated particles was approximately the same, then microstructures resulting in low Ag-110m retention may have existed prior to irradiation. We suggest this scenario of a relatively stable grain structure during irradiation given:

- the unirradiated grain boundary distribution is nearly identical to the grain boundary distribution found in the low-retention, irradiated particle,
- the SiC grain size, at ~1–1.5 μm (Kirchhofer et al., 2013), is relatively large (and, therefore, resistant to change),
- the local particle irradiation temperature (Hawkes et al., 2014) is expected to be, at most, on the order of the SiC layer fabrication temperature 1500 °C (Hunn et al., 2006a,b) where the microstructure developed
- and the irradiation temperature is less than half of the melting point and diffusion in this covalently-bonded material, though enhanced by neutron irradiation damage, is expected to be limited.

If the SiC microstructure associated with low Ag-110m retention truly did not evolve significantly during the irradiation experiment, the possibility exists that changes to fabrication parameters may eliminate or minimize particles with distributions susceptible to Ag-110m release. Additionally, if the preceding discussion is true and significant microstructural evolution did not occur, then the two irradiated grain boundary distributions in Fig. 5b also suggests that considerable particle-to-particle variation in the SiC microstructure exists. (If differences in the grain boundary distributions shown in Fig. 5b were due to local variations in microstructure within the SiC layer of a given particle, then one would not expect to see a difference in release behavior, provided the temperature of the two particles were similar.)

3.3. Influences of variant type and irradiation parameters on fission product precipitate/grain boundary-type associations

In all particles studied, relatively few grain boundaries had fission product precipitates associated with them. Generally, less than ~1% of the SiC grain boundaries had one or more fission product precipitates associated with them. The grain boundary type associated with each grain boundary fission product precipitate was determined in the areas analyzed with PED. The results are plotted in Fig. 6. (Only a few fission product precipitates were found at the IPyC/SiC interface of the high retention Variant 1, particle, AGR1-531-031; therefore, this particle was not included in Fig. 6.) Distributions for the two particles exhibiting Ag-110m release are quite similar with slight differences in the fraction of precipitates on random, high angle grain boundaries and CSL-related grain boundaries, Fig. 6. Most fission products are associated with random, high-angle grain boundaries as reported previously

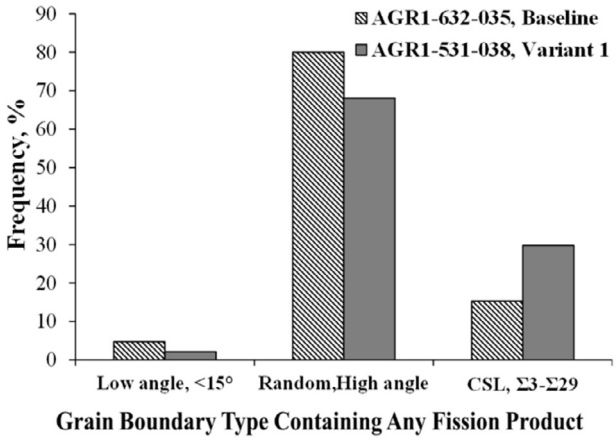

Fig. 6. Distribution of fission product precipitates associated with low-angle, random, high-angle, and CSL-related grain boundaries are compared.

Lillo et al. (2016). Only a few fission products were found on CSL-related grain boundaries and even fewer were found on low-angle grain boundaries. These results can be explained using relative grain boundary energy (Lillo et al., 2016). Diffusivity is related to grain boundary energy, with higher energy grain boundaries exhibiting higher diffusivities (Peterson, 1983). Random, high-angle grain boundaries typically exhibit the highest energy and, therefore, the highest grain boundary diffusivity. The CSL-related grain boundaries in these particles generally consist mostly of Σ3, Σ9 and Σ27 grain boundaries (Fig. 3c), which are generally low energy boundaries. Therefore, fission product transport along these grain boundaries is likely minimal and the fission product concentration may never attain a sufficiently high value to allow for the nucleation and growth of a fission product precipitate. Similarly, grain boundary diffusion in low-angle grain boundaries may be described by dislocation pipe diffusion along the individual dislocations of the grain boundary (Peterson, 1983; Turnbull and Hoffman, 1954). Again, the boundary energy is low, fission product diffusivity is expected to be low and fission product concentrations may not attain sufficient levels for fission product precipitation.

The distribution in Fig. 6 can be broken down further and separated by fission product elements contained in the precipitates based on a qualitative assessment of probe- based energy dispersive X-ray spectrometry. These results can then be correlated with the grain boundary data obtained with PED. The results are presented in Table 2.

The only fission product or transuranic elements with significant concentrations (i.e., > 0.2 atomic %), as determined with energy dispersive X-ray spectroscopy (EDS), were palladium, silver, and uranium. (The source and transport mechanism of uranium in SiC is not fully resolved at this time but warrants further investigation.) It was

Table 2
Fission product elements and grain boundary types associated with grain boundary precipitates.

TRISO Particle	Fission product constituents			
	Pd Only, %*	Ag Only, %*	Pd + Ag, %*	Pd + U, %*
AGR1-632-035, 80% Ag Retention, 1070 °C, 2.4 × 10^{25} n/m²				
Low Angle, < 15°	7.5 (4)	0 (0)	0 (0)	0 (0)
CSL-related	18.9 (10)	0 (0)	20.0 (1)	13.3 (2)
Random, High Angle	73.6 (39)	100 (12)	80.0 (4)	86.7 (13)
AGR1-531-038, 19% Ag Retention, 1040 °C, 3.6 × 10^{25} n/m²				
Low Angle, < 15°	3.2 (1)	0 (0)	0 (0)	0 (0)
CSL-related	22.6 (7)	100 (1)	33.3 (1)	41.7 (5)
Random, High Angle	74.2 (23)	0 (0)	66.7 (2)	58.3 (7)

* The value in parentheses is the number of fission product precipitates.

frequently difficult to determine the grain boundary type associated with the precipitates due to the three-dimensional grain boundary network present in even these thin (i.e., 70–120-nm thick), FIB-prepared, TEM samples. Therefore, only those for which the grain boundary could be definitively identified are included in Table 2. As a result, the datasets are relatively small and the number of precipitates represented by each fraction in Table 2 has been provided.

Overall, all types of fission products seem to prefer random, high-angle grain boundaries regardless of variant type or compact irradiation conditions. As previously reported Lillo et al. (2016) palladium seems to be capable of precipitating out on any type of grain boundary, while silver-only precipitates seem to be limited mainly to random, high-angle grain boundaries. AGR1-531-038 appears to contain fewer silver-only precipitates, which may be due to a different actual particle temperature compared to AGR1-632-035 or the differences in the grain boundary distributions shown in Fig. 3 (e.g., the boundaries susceptible to silver-only precipitates may not be present in as high of numbers as in AGR1-632-035). However, considering the relatively small sample size, the fission product precipitate associations with various grain boundary types appear to be quite similar for the two particles shown in Table 2. This behavior is expected since fission product/grain boundary type associations are mainly dependent on grain boundary energy. Irradiation conditions (i.e., particle temperature, burnup, and neutron fluence) are expected to have minimal effect on grain boundary energy. However, irradiation conditions are expected to have a larger effect on transport kinetics due to excess vacancy generation from neutron damage. Provided grain boundary diffusion is the main mechanism for fission product precipitate formation, the maximum distance away from the fuel kernel for any given precipitate type, for a given time and temperature, will be a function of the distribution and number of random, high-angle grain boundaries and the associated fission product diffusivity in those boundaries.

4. Conclusions

The grain boundary distributions and fission product precipitation behavior in irradiated TRISO fuel particles from the AGR-1 experiment were compared. Two particles exhibited relatively high (i.e., > 80%) Ag-110m retention, while a third exhibited very low Ag-110m retention (i.e., < 19%). The following conclusions can be made based on this study:

- TRISO particles exhibiting high Ag-110m retention (i.e., > 80%) tended to contain more twin-related grain boundaries (Σ3, Σ9 and Σ27) than the low Ag-110m retention particle.
- The TRISO particle exhibiting low Ag-110m retention (i.e., < 19%) contained a higher fraction of random, high-angle grain boundaries which are high diffusivity pathways. Therefore, it was concluded that higher fractions of random, high-angle grain boundaries aid in the release of Ag-110m.
- The inverse dependence of Ag-110m retention on the fraction of random, high-angle grain boundaries is consistent with grain boundary percolation theory. Below a critical threshold of about 20% random, high-angle grain boundaries, there are insufficient numbers of interconnected, high-diffusivity SiC grain boundary transport paths for Ag-110m to allow significant release of Ag-110m under the conditions of temperature and time in the AGR-1 experiment.
- Above a critical value of about 48% random, high-angle grain boundaries, there are sufficient interconnected, high-diffusivity paths to accomplish complete release of Ag-110m under the conditions of temperature and time in the AGR-1 experiment.
- Comparison of irradiated and as-fabricated grain boundary distributions of the same TRISO particle fuel variant revealed:
- significant differences in the CSL-related and low angle grain boundary fractions in baseline particles
  - o significant differences in the random, high angle grain boundary fraction of the high Ag-110m retention, Variant 1 particle, (AGR1-531-031).
  - o grain boundary distributions in the low Ag-110m retention Variant 1 particle (AGR1-531-038) were very similar to the as-fabricated (unirradiated) Variant 1 particle, suggesting that, microstructures more susceptible to Ag-110m transport may have existed in the SiC layer prior to irradiation, provided significant microstructural evolution during irradiation did not occur.
- The association of fission product precipitates with specific grain boundary types showed a preference for random, high-angle grain boundaries for all TRISO particle variant types.
- A breakdown of fission product precipitates by element present showed palladium was capable of precipitating on low-angle, CSL-related and random, high-angle grain boundaries while silver-only precipitates were mainly confined to random, high-angle grain boundaries.

The work discussed here lead to the following recommendations:

- Methods are needed to determine actual TRISO particle temperature and neutron fluence.
- Additional studies are needed to verify the relationship between Ag-110m release fraction and the high-angle grain boundary fraction (Fig. 4).
- Additional analyses of as-fabricated (unirradiated) TRISO particles of Variant 1 and baseline varieties are needed to determine the particle-to-particle variations in the grain boundary distributions.
- Ancillary studies are needed to determine the influence of fabrication conditions for the SiC layer on SiC grain boundary distributions, especially the high-angle grain boundary fraction, to produce SiC microstructures more resistant to Ag-110m release.
- Supporting analyses and characterization are needed to further understand the association of fission product precipitates with particular grain boundary types.
- Study of fission product precipitates in the SiC layer from TRISO particles subjected to accident conditions (temperatures up to 1800 °C) as they may provide further insight into Ag transport and the influence of SiC microstructure.
- Study of the source and transport of U through the SiC layer.

Acknowledgments

This work was sponsored by the United States Department of Energy, Office of Nuclear Energy, under United States Department of Energy Idaho Operations Office Contract DE-AC07-05ID14517, as part of the Advanced Gas Reactor Development Program and as part of an Advanced Test Reactor Nuclear Science User Facilities Rapid Turnaround Experiment.

References

ASTM Standard E2627-13, 2013. Standard Practice for Determining Average Grain Size Using Electron Backscatter Diffraction (EBSD) in Fully Recrystallized Polycrystalline Materials. ASTM International, West Conshohocken PA www.astm.org.

Balluffi, R.W., 1982. Grain boundary diffusion mechanisms in metals. Metall. Trans. A 13A, 2069–2095.

Coward, R.A., Winkler, C.R., Hanson, W.A., Jablonski, M.L., Taheri, M.L., 2015. Transmission electron microscopy investigation of Ag diffusion mechanisms in β-SiC. J. Nucl. Mater. 457, 298–303.

Demkowicz, P.A., Hunn, J.D., Morris, R.N., Van Rooyen, I.J., Gerczak, T., Harp, J.M., Ploger, S.A., 2015. AGR-1 Post Irradiation Examination Final Report, INL/EXT-15-36407, Revision 0.

Demkowicz, P.A., Hunn, J.D., Ploger, S.A., Morris, R.N., Baldwin, C.A., Harp, J.M., Winston, P.L., Gerczak, T.J., van Rooyen, I.J., Montgomery, F.C., Silva, C.M., 2016. Irradiation performance of AGR-1 high temperature reactor fuel. Nucl. Eng. Design 306, 2–13.

Deng, J., Ko, H., Demkowicz, P., Morgan, D., Szlufarska, I., 2015. Grain boundary diffusion of Ag through polycrystalline SiC in TRISO fuel particles. J. Nucl. Mater. 467, 332–340.

Dholabhai, P.P., Aguiar, J.A., Wu, L., Holesinger, T.G., Aoki, T., Castro, R.H.R., Uberuaga, B.P., 2015. Structure and segregation of dopant–defect complexes at grain boundaries in nanocrystalline doped ceria. Phys. Chem. Chem. Phys. 17, 15375–15385.
Engelhard, J., Krüger, K., Gottaut, H., 1975. Investigations of the impurities and fission products in the AVR coolant at an average hot temperature of 950 °C. Nucl. Eng. Design 34, 85.
Hawkes, G.L., Murray, P.E., 2014. AGR-1 daily as-run thermal analyses. Idaho National Laboratory ECAR-968 Rev 4, INL/MIS-11-23668.
Herrmann, G., Gleiter, H., Baro, G., 1976. Investigation of low energy grain boundaries in metals by a sintering technique. Acta Metall. 24, 353–359.
Hunn, J.D., Lowden, R.A., Data Compilation for AGR-1 Baseline Coated Particle Composite LEU01-46T, ORNL/TM-2006/019, Revision 1, April 2006.
Hunn, J.D., Lowden, R.A., Data compilation for AGR-1 variant 1 coated particle composite LEU01-47T, ORNL/TM-2006/020, Revision 1, April 2006.
Kirchhofer, R., Hunn, J.D., Demkowicz, P.A., Cole, J.I., Gorman, B.P., 2013. J. Nucl. Mater. 432, 127–134.
Lillo, T.M., Van Rooyen, I.J., 2015. Associations of Pd, U and Ag in the SiC layer of neutron-irradiated TRISO fuel. J. Nucl. Mater. 460, 97–106.
Lillo, T.M., Van Rooyen, I.J., 2016. Influence of SiC grain boundary character on fission product transport in irradiated TRISO fuel. J. Nucl. Mater. 473, 83–92.
Lillo, T.M., Van Rooyen, I.J., Wu, Y.Q., 2016. Precession electron diffraction for SiC grain boundary characterization in unirradiated TRISO fuel. Nucl. Eng. Design 305, 277–283.
Lòpez-Honorato, E., Yang, D., Tan, J., Meadows, P.J., Xiao, P., 2010. Silver diffusion in coated fuel particles. J. Am. Ceram. Soc. 93, 3076–3079.
Maclean, H.J., 2004. Silver Transport in CVD Silicon Carbide. Ph.D. thesis. Department of Nuclear Engineering MIT, Boston.
Malherbe, J.B., 2013. Diffusion of fission products and radiation damage in SiC. J. Phys. D: Appl. Phys. 46, 473001.
Minato, K., Ogawa, T., Kashimura, S., Fukuda, K., Shimizu, M., Tayama, Y., Takahashi, I., 1990. J. Nucl. Mater. 172, 184–196.
Nabielek, H., Brown, P.E., 1975. The Release of Silver-110m in High Temperature Reactors: Technical Note, OECD Dragon Project 657, 370.
Nabielek, H., Brown, P.E., Offermann, P., 1977. Nucl. Technol. 35, 483–493.
O'connell, J.H., Neethling, J.H., 2014. Ag transport in high temperature neutron irradiated 3C-SiC. J. Nucl. Mater. 445, 20–25.
Peterson, N.L., 1983. Grain-boundary diffusion in metals. Int. Met. Rev. 28, 65–91.
Priester, L., 1989. Geometrical specialty and special properties of grain boundaries. Rev. Phys. Appl. 24, 419–438.
Rabone, J., Lòpez-Honorato, E., 2015. Density functional theory metadynamics of silver, cesium and palladium diffusion at β-SiC grain boundaries. J. Nucl. Mater. 458, 56–63.
Randle, V., 1997. The role of grain boundary plane in cubic polycrystals. Acta Mater. 46, 1459–1480.
Schuh, C.A., Minich, R.W., Kumar, M., 2003. Connectivity and percolation in simulated grain-boundary networks. Philos. Mag. 83, 711–726.
Sutton, A.P., Vitek, V., 1983. On the structure of tilt grain boundaries in cubic metals. III. Generalizations of the structural study and implications for the properties of grain boundaries. Philos. Trans. R. Soc. London, Ser. A 309, 55–68.
Turnbull, D., Hoffman, R.E., 1954. The effect of relative crystal and boundary orientations on grain boundary diffusion rates. Acta Metall. 2, 419–426.
van Rooyen, I.J., Dunzik-Gougar, M.L., Van Rooyen, P.M., 2014. Silver (Ag) transport mechanisms in SiC layer of TRISO coated particles: a critical review. Nucl. Eng. Design 271, 180–188 (Also presented at the HTR2012 Tokyo 28 October–1 November 2012, Paper HTR-3-040).
Van Rooyen, I.J., Dunzik-Gougar, M.L., Van Rooyen, P.M., 2014. Nucl. Eng. Design 271, 180–188.
Van Rooyen I.J., Nabielek H., Neethling J.H., Kania M.J., Petti D.A., 2014. Progress in solving the elusive Ag transport mechanism in TRISO coated particles: What's new? HTR2014-3-1261. In: Proceedings of the HTR2014, Weiha, China, October 27–31.
Van Rooyen, I.J., Van Rooyen, P.M., Dunzik-Gougar, M.L. The effect of high temperature annealing on the grain characteristics of a thin chemical vapor deposition silicon carbide layer. Microsc. Microanal. 19 (2) 1948–1949, doi: 10.1017/S1431927613011732, published online: 09 October 2013 (also presented at the Microscopy & Microanalysis Conference, Indianapolis, August 4–8, 2013).
Van Rooyen, I.J., Neethling, J.H., Henry, A., Janzen, E., Mokoduwe, S.M., Janse Van Vuuren, A., Olivier, E., 2012. Effects of phosphorous-doping and high temperature annealing on CVD grown 3C SiC. Nucl. Eng. Design 251, 191–202.
Van Rooyen, I.J., Lillo, T.M., Wu, Y.Q., 2014. J. Nucl. Mater. 446, 178–186.
Van Rooyen, I.J., Janney, D.E., Miller, B.D., Demkowicz, P.A., Riesterer, J., 2014. Nucl. Eng. Design 271, 114–122.
Wolf, D., 1990. Structure-energy correlation for grain boundaries in F.C.C metals – III. Symmetrical tilt boundaries. Acta Metall. Mater. 38, 781–790.
Wu, L., Aguiar, J.A., Dholabhai, P.P., Holesinger, T.G., Aoki, T., Uberuaga, B.P., Castro, R.H.R., 2015. Interface Energies of nanocrystalline doped ceria: effects of manganese segregation. J. Phys. Chem. C. 119 (49), 27855–27864.